

Comparison of the empty electronic states of $\text{Bi}_2\text{Sr}_2\text{CaCu}_2\text{O}_8$ (001) and $\text{Bi}_2\text{Sr}_2\text{CuO}_6$ (001) at 60 and 300 K

T. J. Wagener, Y.-J. Hu, M. B. Jost, and J. H. Weaver

Department of Chemical Engineering and Materials Science, University of Minnesota, Minneapolis, Minnesota 55455

Y. F. Yan, X. Chu, and Z. X. Zhao

Institute of Physics, P.O. Box 603, Chinese Academy of Science, Beijing, China

(Received 23 April 1990)

Inverse photoelectron spectroscopy has been used to study the unoccupied electronic states of $\text{Bi}_2\text{Sr}_2\text{CaCu}_2\text{O}_8$ (001) and $\text{Bi}_2\text{Sr}_2\text{CuO}_6$ (001) at 60 and 300 K. Both compounds exhibit low emission between E_F and $E_F + 2$ eV derived from Cu $3d$ -O $2p$ and Bi $6p$ -O $2p$ hybrids and structure centered at ~ 4 and 9.5 eV that can be attributed to empty Bi $6p$ and Sr $4d$ levels. Results for $\text{Bi}_2\text{Sr}_2\text{CaCu}_2\text{O}_8$ show additional structure near $E_F + 10$ eV because of contributions from Ca $3d$ levels. Plasmons are found for both compounds at 15 and 21.2 eV. Off-normal studies of $\text{Bi}_2\text{Sr}_2\text{CaCu}_2\text{O}_8$ (001) at 60 K showed O $2p$ holes with $p_{x,y}$ character. Results obtained at 300 K showed decreased O $2p$ hole emission and increased Cu $3d^{10}$ emission for both $\text{Bi}_2\text{Sr}_2\text{CaCu}_2\text{O}_8$ and $\text{Bi}_2\text{Sr}_2\text{CuO}_6$ compared with the 60 K results.

I. INTRODUCTION

A great deal of attention has been placed on elucidating the mechanism(s) responsible for high- T_c superconductivity. Frequently, comparisons have been made among similar compounds that exhibit very different T_c 's. For instance, $\text{La}_{2-x}\text{Sr}_x\text{CuO}_4$ has O $2p$ hole states and $T_c \sim 32$ K, while the antiferromagnetic insulator La_2CuO_4 does not.¹ In general, $R\text{Ba}_2\text{Cu}_3\text{O}_{7-x}$ systems exhibit superconductivity at 93 K and have O $2p$ hole states for $x < 0.5$, but the O $2p$ hole states are quenched for $x > 0.5$ and superconductivity is not observed (R denotes the rare-earth elements except Tb, Ce, and Pr).¹⁻⁴ Intriguingly, O $2p$ hole states have been reported for $\text{PrBa}_2\text{Cu}_3\text{O}_{7-x}$, but high-temperature superconductivity has not been found.⁴⁻⁵ For $\text{YBa}_2\text{Cu}_3\text{O}_{7-x}$, 10% substitution of Zn for Cu suppresses superconductivity without apparently altering the O $2p$ hole states.⁶ Hence O $2p$ holes are necessary, but not sufficient, for high- T_c superconductivity.⁴

Variations in T_c have also been observed for the $\text{Bi}_2\text{Sr}_2\text{Ca}_{n-1}\text{Cu}_n\text{O}_y$, where n represents the number of CuO_2 planes in each crystal sublattice. Transition temperatures of ~ 10 , 85, and 110 K have been obtained for the $n = 1, 2$, and 3 compounds, respectively.⁷ Photoemission studies have shown similar core-level and valence-band structure for the $n = 1$ and 2 compounds,⁸ with slightly higher relative emission near E_F for $n = 2$ due to the second CuO_2 plane.^{8,9} They also showed that these compounds cleave between Bi-O layers.⁸

In this paper, we show that the empty electronic states of $\text{Bi}_2\text{Sr}_2\text{CaCu}_2\text{O}_8$ (001) and $\text{Bi}_2\text{Sr}_2\text{CuO}_6$ (001) are nearly indistinguishable, as revealed by tunable-energy inverse photoelectron spectroscopy (IPES). Temperature-dependent studies were undertaken, in part because of the proposed structural phase transition at ~ 210 K,¹⁰ and

they show increased O $2p$ hole emission and decreased Cu $3d^{10}$ emission at 60 K. No temperature-dependent changes were observed for the Bi, Sr, and Ca levels, and this indicates that the changes were confined to the CuO_2 planes. Momentum-resolved inverse photoelectron spectroscopy (KRIPES) results acquired at 60 K for off-normal incidence for $\text{Bi}_2\text{Sr}_2\text{CaCu}_2\text{O}_8$ (001) showed O $2p$ hole states with $p_{x,y}$ character.

II. EXPERIMENT

The IPES experiments were conducted in a four-chamber system operating at a base pressure of 1×10^{-10} Torr.¹¹ A collimated monoenergetic electron beam (current ~ 10 μA , beam spot 1×5 mm^2) was provided by a Pierce-type electron gun manufactured by Kimball Physics. The angular divergence of the electron beam ($< 3^\circ$ at 25 eV) gave a momentum resolution of ~ 0.1 \AA^{-1} . Emitted photons were dispersed by an $f/3.5$ grating onto a position-sensitive detector. The combined energy resolution of the spectrometer (electrons and photons) was 0.3–1.0 eV for photons detected at energies of 10–44 eV. The samples were cooled to 60 K with a closed-cycle helium refrigerator via a copper braid. The temperature was determined with a Au–0.07 at. % Fe versus chromel thermocouple attached to the same holder.

Single crystals of $\text{Bi}_2\text{Sr}_2\text{CaCu}_2\text{O}_8$ (001) and $\text{Bi}_2\text{Sr}_2\text{CuO}_6$ (001) were prepared by grinding high-purity reagents with stoichiometric ratios for [Bi]:[Sr]:[Ca]:[Cu] of 2:2:2:3 and 2:2:0:3, respectively.¹² After sintering at 850 $^\circ\text{C}$, they were reground and placed in Al_2O_3 crucibles. Following annealing at 1050 $^\circ\text{C}$ (2 h) and 950 $^\circ\text{C}$ (12 h), they were cooled to 850 $^\circ\text{C}$ at a rate of 2 $^\circ\text{C}/\text{h}$, then cooled to room temperature at a rate of 50 $^\circ\text{C}/\text{h}$. The stoichiometries were determined to be $\text{Bi}_2\text{Sr}_2\text{CaCu}_2\text{O}_8$ (2:2:1:2) and $\text{Bi}_2\text{Sr}_2\text{CuO}_6$ (2:2:0:1). The superconducting transition

temperature for the 2:2:1:2 samples was measured to be 85 K, while the 2:2:0:1 samples were not superconducting. The single crystals shared a common [001] axis but had randomly-oriented *a-b* domains.

The single crystals ($8 \times 8 \times 0.25$ mm³) were mounted on Cu posts with conducting epoxy and were covered with an epoxy bead. They were transferred into the measurement chamber after bakeout, and the beads were pried off *in situ* at 60 or 300 K to expose mirrorlike (001) surfaces. Immediately after cleaving, a surface-sensitive KRIPES spectrum was acquired with an incident electron energy of 18 eV. Periodic checks showed no changes that could be related to electron bombardment or residence in vacuum. Low-energy electron-diffraction (LEED) studies showed multiple domains that were randomly oriented about the *c* axis, i.e., [001].

III. RESULTS AND DISCUSSIONS

A. IPES of Bi₂Sr₂CaCu₂O₈ and Bi₂Sr₂CuO₆ at 60 K

In Fig. 1 we present photon-distribution curves (PDC's) acquired at 60 K from 2:2:1:2 (solid lines) and 2:2:0:1 (dashed lines). These spectra are referenced in energy to the Fermi level E_F and the incident electron energies E_i are referenced to E_F . All spectra were acquired with incident electrons normal to the (001) surfaces, and a constant photon-energy feature at $h\nu=21.2$ eV is marked with arrows, and it can be seen to move to the right in Fig. 1 as E_i is increased. The spectra for 2:2:1:2 and 2:2:0:1 are renormalized to the emission intensity at $h\nu=21.2$ eV to facilitate comparison. Analogous IPES spectra have been shown previously¹³ for polycrystalline 2:2:1:2.

The spectra in Fig. 1 reveal low emission for states from E_F to E_F+2 eV for both 2:2:1:2 and 2:2:0:1. These states are due to the Cu 3*d*-O 2*p* and Bi 6*p*-O 2*p* hybrids.¹⁴⁻¹⁶ The shoulder at E_F+4 eV is attributed to higher-lying Bi 6*p* levels that are predicted to be 2.5 eV above E_F ,¹⁴⁻¹⁶ i.e., ~ 1.5 eV closer to E_F than observed. We will discuss the states near E_F in Fig. 2.

The strong emission observed between E_F+6 and 14 eV in Fig. 1 is due to empty Sr 4*d*-derived and Ca 3*d*-derived levels. Comparison of spectra acquired at $E_i=35$ and 39 eV indicates a significant increase in emission from the feature centered at ~ 9.5 eV above E_F . Since this enhancement occurs for both compounds, we attribute it to the Sr 4*p*-*d* giant-dipole-resonant transition. Such empty-state resonances have been observed for many of the early transition elements, and they have been discussed in detail for Sc.¹⁷ A further increase in E_i to 43 or 47 eV produces additional enhancement for 2:2:1:2 that can be ascribed to the Ca 3*p*-3*d* giant-dipole-resonant transition (centered at ~ 10 eV with maximum intensity at $E_i=45$ eV). The higher-energy resonance for Ca compared to Sr is expected since the binding energy of the Ca 3*p* core level is ~ 5 eV greater than that of the Sr 4*p* core level.¹⁸ The empty-state values of ~ 9.5 and 10 eV above E_F for the Sr 4*d* and Ca 3*d* bands are consistent with the highly ionic character of the cuprate oxides [compare to centroids for metallic Sr 4*d* and Ca 3*d* bands

at ~ 5 eV (Ref. 19) and ~ 6 eV (Ref. 20) above E_F].

A constant photon-energy feature centered at $h\nu=21.2$ eV can be seen in Fig. 1 for both 2:2:1:2 and 2:2:0:1. Although not shown, another constant photon-energy feature appears at $h\nu=15$ eV. In a previous IPES study of polycrystalline 2:2:1:2,¹³ we attributed the constant photon features at 15 and 21.2 eV to radiative plasmon losses. These plasmon loss features have a full width at half maximum (FWHM) of 3 eV, and they have similar properties to the plasmon-loss features reported for Sb.²¹ As shown in Fig. 1, the 21.2-eV plasmon-loss feature is indistinguishable for 2:2:1:2 and 2:2:0:1, as is the $h\nu=15$ -eV feature. The energies of the two plasmon features differ by a factor of 1.4, suggesting that the lower-energy feature can be attributed to a surface plasmon. Since the 2:2:1:2 and 2:2:0:1 compounds have similar planar character and electron densities, it is not surprising that they exhibit similar bulk plasmon losses. Furthermore, since both cleave between Bi-O planes, they will have similar surface properties, and the radiative decay of the surface plasmons should be equivalent.

In Fig. 2 we compare emission from the empty electronic states of 2:2:1:2 (left panel) and 2:2:0:1 (right panel) between E_F and E_F+4 eV. The spectra were acquired within 30 min of cleaving at 60 K with normal incident electrons of $E_i=16$ eV (dashed lines) and 18 eV (solid

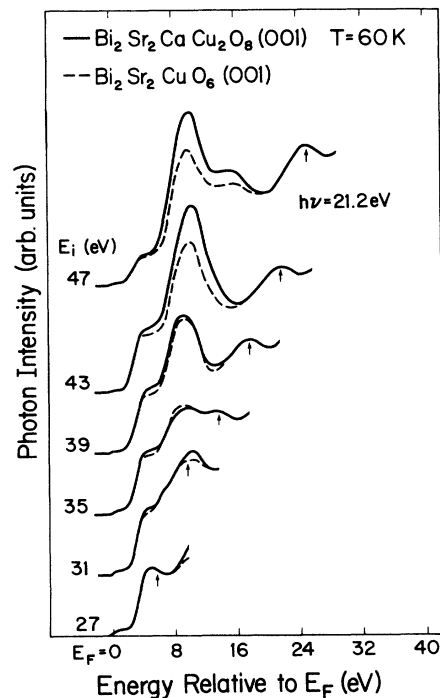


FIG. 1. Normal incidence IPES spectra as a function of incident electron energy E_i for 2:2:1:2 (solid line) and 2:2:0:1 (dashed line). Cu 3*d*-O 2*p* and Bi 6*p*-O 2*p* states lie between E_F and E_F+2 eV, the Bi 6*p* levels produce structure at E_F+4 eV, and the Sr 4*d* levels are centered at $E_F+9.5$ eV. The spectra for the two compounds differ for $E_i=43$ and 47 eV because the Ca 3*p*-3*d* giant dipole resonance in 2:2:1:2 highlights the Ca 3*d* states. The constant photon-energy feature at $h\nu=21.2$ eV represents radiative plasmon decay.

lines). The four IPES spectra of Fig. 2 were normalized to constant height at $E_F + 4$ eV. (Typically, we normalize to electron doses, but the samples were electrically grounded during the low-temperature studies. Normalization at a fixed energy allows comparisons for a given material, but quantitative comparisons between 2:2:1:2 and 2:2:0:1 should not be made.) These IPES spectra show the well-defined E_F cutoff characteristic of the Bi-Sr-(Ca)-Cu-O compounds. The cutoff appears more distinctly for these compounds than for La-Sr-Cu-O and Y-Ba-Cu-O because of the added Bi $6p$ -O $2p$ states at E_F .⁴

In Fig. 2, we overlay the $E_i = 16$ - and 18-eV spectra to emphasize the enhanced structure between E_F and $E_F + 2$ eV that occurs for $E_i \sim 18$ eV in all of the cuprate superconductors.⁴ This enhancement has been attributed to an O-derived resonance whereby the incident electron beam induces O $2s$ -O $2p$ transition. Radiative decay channels of the core hole, $O(2s^1 2p^6) \rightarrow O(2s^2 2p^5) + h\nu$, couple with the IPES continuum and produce resonant enhancement.²² The differences between the $E_i = 16$ - and 18-eV spectra are shown at the bottom of Fig. 2, multiplied by three for visual comparison. The difference curves show nearly identical O $2p$ hole character for 2:2:1:2 and 2:2:0:1, despite the large differences in transition temperatures (85 versus 10 K). This suggests that there are no

fundamental differences in the O $2p$ hole character for these two Bi-Sr-(Ca)-Cu-O compounds, at least on the energy scale of these measurements.

The inset of Fig. 2 shows inverse-constant final-state (ICFS) curves for 2:2:1:2 (solid line) and 2:2:0:1 (dashed line) taken at a final-state energy of $E_F + 1$ eV. This final-state energy corresponds to the peak in intensity of the empty O $2p$ states. The Fano line shape exhibited by the ICFS curves is consistent with enhancement due to an O $2s$ - $2p$ resonant transition. The ICFS curves are re-normalized to the same background emission between $E_i = 20$ and 21 eV and show that the amount of enhanced emission above background is approximately twice as large for the 2:2:1:2 compound. This suggests greater O $2p$ hole character in the 2:2:1:2 compound. The consequence can be seen in the IPES spectra acquired at $E_i = 18$ eV. Indeed, the peak for 2:2:1:2 occurs clearly at $E_F + 1$ eV whereas 2:2:0:1 has a somewhat flatter distribution between E_F and $E_F + 2$ eV. These results can be related to the existence of two CuO_2 planes in 2:2:1:2 compared to one in 2:2:0:1 and help to verify that the O $2p$ hole states originate in CuO_2 planes. While there are more O $2p$ hole states in 2:2:1:2, their distribution and character is similar for 2:2:1:2 and 2:2:0:1.

B. Off-normal results for $\text{Bi}_2\text{Sr}_2\text{CaCu}_2\text{O}_8$ (001) at 60 K

In Fig. 3 we present off-normal KRIPES spectra taken at $E_i = 16$ eV (left) and $E_i = 18$ eV (right) for $\text{Bi}_2\text{Sr}_2\text{CaCu}_2\text{O}_8$ (001). The PDC's were acquired at 60 K immediately after cleaving. The angle between the incident electrons and the surface normal is represented by θ , as labeled. The $\theta = 0^\circ$ spectrum is repeated as a dashed line overlaid on each off-normal curve. Since the samples have randomly oriented domains aligned along the c axis, the off-normal spectra do not follow any specific direction within the (001) plane of k space. Since $\text{Bi}_2\text{Sr}_2\text{CaCu}_2\text{O}_8$ is a two-dimensional compound, the initial state is determined by the momentum parallel to the surface. Therefore, the $\theta = 0^\circ$ spectrum represents Γ , and spectra taken at increased θ represent a fixed radial distance (but arbitrary azimuthal direction) in the (001) plane.

Figure 3 shows increased emission near E_F for the $\theta = 10^\circ$ spectra. If those spectra sampled the zone along [110] or [100], then the $\theta = 10^\circ$ spectra would represent either 0.25 Γ -X or 0.35 Γ -M. A KRIPES study by Claessen *et al.*²³ also observed increased emission near E_F at ~ 0.5 Γ -X. We suggest that this increased emission represents Cu $3d$ -O $2p$ hybrids that are expected to cross E_F at ~ 0.3 Γ -X.¹⁴⁻¹⁶ Indeed, angle-resolved photoemission results²⁴⁻²⁶ show this band crossing at 0.33 Γ -X.

For $\theta > 10^\circ$, the increased emission spreads away from E_F and eventually occurs throughout the region between E_F and $E_F + 3$ eV. This increased emission is larger for the $E_i = 18$ -eV spectra, suggesting that it can be associated with the O $2p$ hole character from the CuO_2 planes, even though some of the increase could be related to Bi-O hybrids. Spectra taken at $\theta = 25^\circ$ and 30° show this increased emission to broaden asymmetrically toward E_F , centered near $E_F + 0.75$ eV. For $\theta = 40^\circ$, this structure is

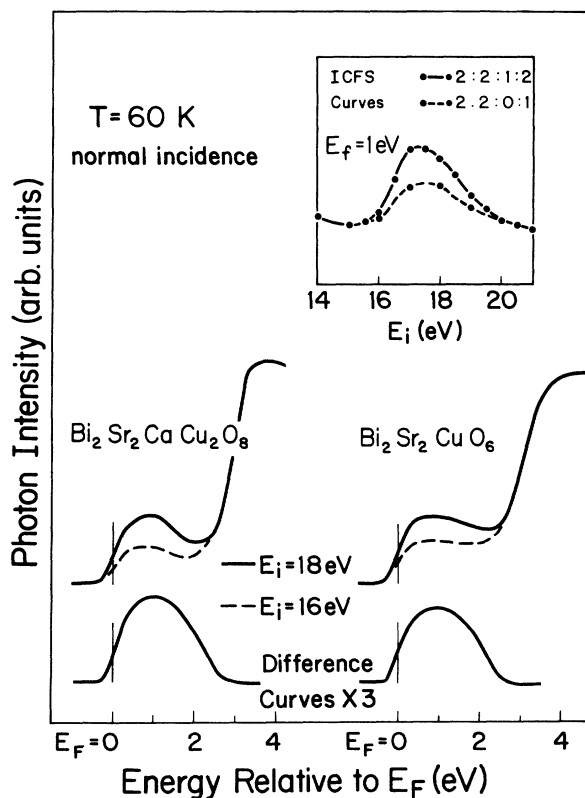


FIG. 2. IPES spectra for 2:2:1:2 and 2:2:0:1 to emphasize the empty states between E_F and $E_F + 4$ eV. Spectra for $E_i = 16$ and 18 eV correspond to off and on the O $2s$ - $2p$ resonant transition. The O $2p$ character is nearly identical for 2:2:1:2 and 2:2:0:1. Inverse-constant final-state energy spectra shown in the inset display a Fano line shape and an enhancement that is twice as large for 2:2:1:2 because of the extra CuO_2 plane.

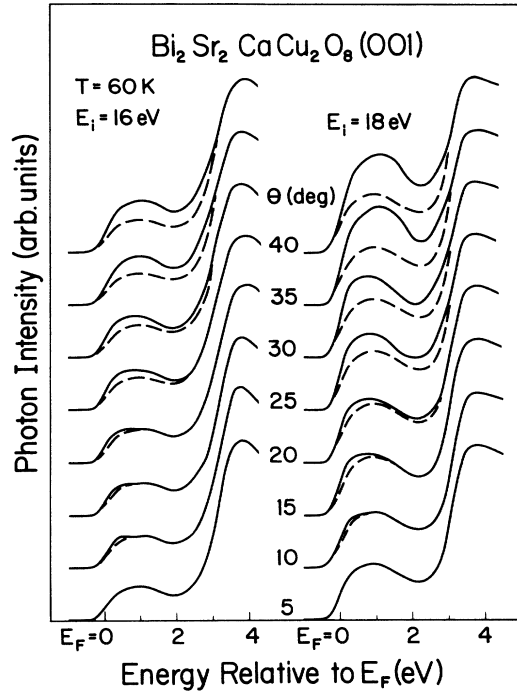


FIG. 3. Off-normal KRIPES spectra acquired at 60 K for $\text{Bi}_2\text{Sr}_2\text{CaCu}_2\text{O}_8$ (001). The $\theta=0^\circ$ spectrum is shown dashed and is overlaid on each off-normal curve to emphasize changes. Increased O 2p hole emission is found for increased angle θ , consistent with $p_{x,y}$ character.

centered near E_F+1 eV. Band-structure calculations predict the Cu $3d$ -O $2p$ antibonding hybrids to disperse across E_F along Γ - X and peak near E_F+2 eV at the X point.¹⁴⁻¹⁶ If this study was conducted along Γ - X , then the $\theta=25^\circ$ and 30° spectra would represent ~ 0.7 Γ - X and $\theta=40^\circ$ spectra would represent the X point. We suggest that the observed behavior qualitatively parallels that predicted by theory, showing that the Cu $3d$ -O $2p$ antibonding hybrids have dispersive character along the a - b plane. Similar conclusions for $\text{Bi}_2\text{Sr}_2\text{CaCu}_2\text{O}_8$ have been reached by Himpsel *et al.*²⁷ based on optical absorption studies.

C. IPES of $\text{Bi}_2\text{Sr}_2\text{CaCu}_2\text{O}_8$ and $\text{Bi}_2\text{Sr}_2\text{CuO}_6$ at 300 K

In Fig. 4, we show spectra that represent the temperature-dependent empty electronic states of 2:2:1:2 and 2:2:0:1. The bottom panel compares the 60-K (solid lines) and 300-K (dashed lines) IPES spectra taken at $E_i=16$ and 18 eV, normalized to emission at E_F+4 eV. These spectra were obtained from samples cleaved at the measurement temperature. Identical spectra were obtained from samples cleaved at 60 K and warmed to 300 K, or vice versa. Difference curves are shown in the top panel, with the solid and dashed lines representing the differences in the $E_i=16$ - and 18-eV spectra, respectively. Unfortunately, the experimental resolution was ~ 0.4 eV and changes related to the development of the superconducting gap could not be detailed.²⁴

Figure 4 reveals increased emission between E_F and E_F+2 eV and decreased emission between E_F+2 and 4

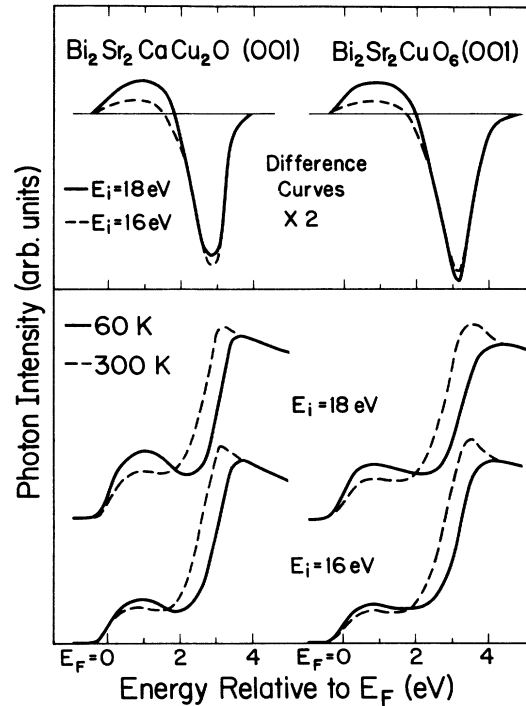


FIG. 4. Temperature-dependent empty-state emission for $\text{Bi}_2\text{Sr}_2\text{CaCu}_2\text{O}_8$ and $\text{Bi}_2\text{Sr}_2\text{CuO}_6$. As can be seen in the difference curves, cooling from 300 to 60 K gives rise to increased emission near 1 eV that we attribute to O states and decreased emission near 3.2 eV that we attribute to d states.

eV at 60 K for both 2:2:1:2 and 2:2:0:1. No temperature-dependent empty electronic state changes were observed above E_F+4 eV. Comparison of the $E_i=16$ - and 18-eV spectra indicates that the increased emission centered at E_F+1 eV can be associated with O 2p character since the changes are larger for incident electron energies near the O 2s threshold energy. The absence of such a dependency on E_i suggests that structures centered at $E_F+2.8$ eV and $E_F+3.2$ eV for 2:2:1:2 and 2:2:0:1, respectively, are not related to changes in O 2p-derived features.

The character of the room-temperature feature at $E_F+2.8$ eV in 2:2:1:2 has been the focus of recent speculation. IPES results by Drube *et al.*²⁸ showed its magnitude to be somewhat cleave dependent, and they attributed it to either localized Cu $3d$ levels or to Bi $6p$ levels. Pattnaik and News²⁹ discussed this feature within the framework of a heavy-fermion normal state and attributed it to a localized Cu $3d$ level. Since x-ray photoemission spectroscopy (XPS) studies of $\text{Bi}_2\text{Sr}_2\text{CaCu}_2\text{O}_8$ showed the Bi $4f$ emission to be temperature independent,³⁰ it is unlikely that it is due to empty Bi $6p$ levels. Hence, we associate the $E_F+2.8$ -eV feature in 2:2:1:2 with localized Cu $3d$ levels, and attribute the feature at $E_F+3.2$ eV in 2:2:0:1 to the equivalent Cu $3d$ level.

These changes in the empty O and Cu features suggest enhanced charge transfer from the O to the Cu at low temperature, possibly because of a structural transition. Indeed, He *et al.*¹⁰ have observed a discontinuity in the specific heat and changes in x-ray-diffraction images at 210 K for both 2:2:1:2 and 2:2:2:3 Bi-Sr-Ca-Cu-O. They

suggest that these anomalies are consistent with a phase transition occurring in either the CuO_2 or BiO planes. With this in mind, we associate with changes to a structural phase transition in the CuO_2 planes. Note that enhanced charge transfer was also observed for $\text{YBa}_2\text{Cu}_3\text{O}_{7-x}$ whereby increased O $2p$ hole and reduced Cu^{2+} satellite emission was found at 60 K.⁴ He *et al.*³¹ also observed ultrasound anomalies near 170 and 250 K for $\text{YBa}_2\text{Cu}_3\text{O}_{7-x}$.

IV. CONCLUSIONS

We have found decreased O $2p$ hole emission and increased Cu $3d$ emission for IPES spectra acquired at 300 K when compared to equivalent spectra acquired at 60 K. These changes can be explained by a phase transition

occurring in the CuO_2 planes at 210 K. We also find that the empty electronic states for 2:2:1:2 are nearly identical to those for 2:2:0:1 at 60 K. In particular, resonant enhancement of the O $2p$ hole levels showed similar O $2p$ hole character even though $T_c \sim 85$ K for 2:2:1:2 and $T_c \sim 10$ K for 2:2:0:1. However, the O $2s$ - $2p$ resonant enhancement was twice as large for 2:2:1:2 because of the extra CuO_2 plane in the 2:2:1:2 sublattice. Finally, off-normal KRIPES results for $\text{Bi}_2\text{Sr}_2\text{CaCu}_2\text{O}_8$ (001) at 60 K found O $2p$ holes with $p_{x,y}$ character.

ACKNOWLEDGMENTS

Discussions with J. L. Martins are gratefully acknowledged. The work at the University of Minnesota was supported by the Office of Naval Research.

-
- ¹N. Nucker, J. Fink, J. C. Fuggle, P. J. Durham, and W. M. Temmerman, *Phys. Rev. B* **37**, 5258 (1988).
²P. H. Hor, R.L. Meng, Y. Q. Wang, L. Gao, Z. J. Huang, J. Bechtold, K. Forster, and C. W. Chu, *Phys. Rev. Lett.* **58**, 1891 (1987).
³P. Kuiper, G. Kruizinga, J. Ghijsen, M. Grioni, P. J. W. Weijs, F. M. F. de Groot, G. A. Sawatzky, H. Verweij, L. F. Feiner, and H. Petersen, *Phys. Rev. B* **38**, 6483 (1988).
⁴T. J. Wagener, H. M. Meyer, III, Yongjun Hu, M. B. Jost, J. H. Weaver, and K. C. Goretta, *Phys. Rev. B* **41**, 4201 (1990).
⁵N. Nucker, J. Fink, J. C. Fuggle, P. J. Durham, and W. M. Temmerman, *Physica C* **153-155**, 119 (1988).
⁶M. L. den Boer, C.L. Chang, H. Petersen, M. Schaible, K. Reilly, and S. Horn, *Phys. Rev. B* **38**, 6588 (1988).
⁷J. M. Tarascon, W. R. McKinnon, P. Barboux, D. M. Hwang, B. G. Bagley, L. H. Greene, G. W. Hull, Y. LePage, N. Stoffel, and M. Giroud, *Phys. Rev. B* **38**, 8885 (1988).
⁸P. A. P. Lindberg, Z.-X. Shen, B. O. Wells, D. B. Mitzi, I. Lindau, W. E. Spicer, and A. Kapitulnik, *Phys. Rev. B* **40**, 8769 (1989).
⁹H. Eisaku, H. Takagi, S. Uchida, H. Matsubara, S. Suga, M. Nakamura, K. Yamaguchi, A. Misu, H. Namatame, and A. Fujimori, *Phys. Rev. B* **41**, 7188 (1990).
¹⁰Y. He, J. Xiang, X. Wang, A. He, J. Zhang, and F. Chang, *Phys. Rev. B* **40**, 7384 (1989).
¹¹Y. Gao, M. Grioni, B. Smandek, J. H. Weaver, and T. Tyrie, *J. Phys. E* **21**, 489 (1988).
¹²Y. F. Yan, C. Z. Li, J. H. Wang, Y. C. Chang, Q. S. Yang, D. S. Hou, X. Chu, Z. H. Mai, H. Y. Zhang, D. N. Zheng, Y. M. Ni, S. L. Jia, D. H. Shen, and Z. X. Zhao, *Mod. Phys. Lett. B* **2**, 571 (1988).
¹³T. J. Wagener, Y.-J. Hu, Y. Gao, M. B. Jost, J. H. Weaver, N. D. Spencer, and K. C. Goretta, *Phys. Rev. B* **39**, 2928 (1989).
¹⁴M. S. Hybertsen and L. F. Mattheiss, *Phys. Rev. Lett.* **60**, 1661 (1988); L. F. Mattheiss and D. R. Hamann, *Phys. Rev. B* **38**, 5012 (1988).
¹⁵H. Krakauer and W. E. Pickett, *Phys. Rev. Lett.* **60**, 1665 (1988).
¹⁶B. A. Richert and R. E. Allen, *J. Phys. Condens. Mat.* **1**, 9443 (1989).
¹⁷Y.-J. Hu, T. J. Wagener, Y. Gao, and J. H. Weaver, *Phys. Rev. B* **38**, 12 708 (1988).
¹⁸H. M. Meyer, III, D. M. Hill, J. H. Weaver, D. L. Nelson, and C. F. Gallo, *Phys. Rev. B* **38**, 7144 (1988).
¹⁹B. Vasvari, *Rev. Mod. Phys.* **40**, 776 (1968).
²⁰D. J. Mickish, A. B. Kunz, and S. T. Pantelides, *Phys. Rev. B* **10**, 1369 (1974).
²¹W. Drube and F. J. Himpsel, *Phys. Rev. Lett.* **60**, 140 (1988).
²²G. Wendin, *Phys. Scr.* **T27**, 31 (1989).
²³R. Claessen, R. Manzke, H. Carstensen, B. Burandt, T. Buslaps, M. Skibowski, and J. Fink, *Phys. Rev. B* **39**, 7316 (1989).
²⁴C. G. Olson, R. Liu, A.-B. Yang, D. W. Lynch, A. J. Arko, R. S. List, B. W. Veal, Y. C. Chang, P. Z. Jiang, and A. P. Paulikas, *Science* **245**, 731 (1989).
²⁵F. Minami, T. Kimura, and S. Takekawa, *Phys. Rev. B* **39**, 4788 (1989).
²⁶T. Takahashi, H. Matsuyama, H. Katayama-Yoshida, Y. Okabe, S. Hosoya, K. Seki, H. Fujimoto, M. Sato, and H. Inokuchi, *Phys. Rev. B* **39**, 6636 (1989).
²⁷F. J. Himpsel, G. V. Chandrashekar, A. B. McLean, and M. W. Shafer, *Phys. Rev. B* **38**, 11 946 (1988).
²⁸W. Drube, F. J. Himpsel, G. V. Chandrashekar, and M. W. Shafer, *Phys. Rev. B* **39**, 7328 (1989).
²⁹P. C. Pattnaik and D. M. Newns, *Phys. Rev. B* **41**, 880 (1990).
³⁰H. M. Meyer, III, T. J. Wagener, and J. H. Weaver, unpublished temperature-dependent XPS studies of $\text{Bi}_2\text{Sr}_2\text{CaCu}_2\text{O}_8$.
³¹Y. He, B. Zhang, S. Lin, J. Xiang, Y. Lou, and H. Chen, *Int. J. Mod. Phys. F* **1**, 517 (1987); *J. Phys. F* **17**, L243 (1988).